A Time-domain Approach to the 3-omega Heat Conductivity Measurement Method

Bendtsen, Jan Dimon; Leth, John-Josef; Kallesøe, Carsten

Published in:
2022 Australian and New Zealand Control Conference (ANZCC)

DOI (link to publication from Publisher):
10.1109/ANZCC56036.2022.9966983

Publication date:
2022

Document Version
Accepted author manuscript, peer reviewed version

A Time-domain Approach to the 3-omega Heat Conductivity Measurement Method

Jan Bendtsen[1], John Leth[1], Carsten Kallesøe[2]

Abstract— The so-called "3ω method" is a well established method to measure heat conductivity of solids. It is a frequency-based method, in which the ratio between the first and third harmonics of an induced voltage in an electric heater element can be shown to be (inversely) proportional to the thermal conductivity of a solid that the heater is in direct contact with. Commonly, the method utilizes Discrete Fourier analysis in an off-line setting, which is of course perfectly valid when measuring material properties in a static setting.

In this paper we propose to make use of the measurement principle in a dynamic setting. We propose a novel time-domain approach to 3ω measurement, which can easily be implemented in a cheap micro-controller due to its modest memory and sampling rate requirements, and therefore likely to be useful for feedback in control loops or similar applications.

The approach comprises two main elements, a discrete-time signal generator, which provides a steady-state sinusoidal current output, and a standard Luenberger-style state observer designed to estimate the associated third harmonic in the presence of noisy voltage measurements. We prove that the signal generator is robust to numerical inaccuracies. The approach is tested in simulation and on actual laboratory data, showing good agreement with traditional off-line analysis.

I. Introduction

The 3ω method was initially proposed over three decades ago by D.G. Cahill and R.O. Pohl as a highly sensitive way to measure thermal conductivity ([1], [2]), utilizing a microfabricated metal line deposited on the specimen to act as a combined heater/thermometer. Since then, it has been used to measure the thermal diffusivity of liquids ([3]) and solids ([4]) by indirectly heating the specimen using a thin planar metal filament as both a heater and thermometer in thermal contact with the solid of interest [5]. More recently, the method has been adapted to experimental measurement of microbial fouling buildup on submerged surfaces and slow-moving liquid flow rates [6], [?] as well as hydrogen concentration measurement in air [7].

The main advantages of the 3ω-method are minimization of radiation effects and easier acquisition of the temperature dependence of the thermal conductivity than in DC-based measurement techniques. Nonetheless, in spite of its usefulness in measuring material properties, the 3ω method appears curiously unknown in the Control community. This may be due to the fact that the usage thus far have been focused on static measurements.

A common theme among the reported investigations in literature is that the measurements rely on Discrete Fourier Transform (DFT)-based analysis. Even though the signal frequency content is quite limited, measurement series are typically generated using high-quality sinusoidal input signals provided by expensive function generators and acquired as high-resolution data at high sampling rates using expensive data acquisition equipment as well—see basically all of the aforementioned references. The frequency analysis is then carried out off-line, and the relevant parameters are estimated a posteriori.

However, it would appear that the 3ω method could potentially find new utilization in the context of measurements on dynamical systems in addition to the aforementioned static measurements. In particular, slowly varying variables—and by slowly, we mean slowly compared to the thermodynamical characteristics of the materials involved in the measurement setup, as will be made clear in the sequel—could be measured and used in dynamic contexts such as closed-loop control or fault detection applications, if only the off-line data analysis requirement could be removed. In addition, it would be advantageous for practical applications, if the hardware requirements could be relaxed and the measurement setup could be implemented using cheap, off-the-shelf microprocessor hardware with limited processing speed, memory requirements, and signal generation capabilities.

This paper thus attempts to lay the groundwork for making the 3ω method useful in a dynamical systems context. The main contribution of this paper is therefore to propose a time-domain periodic signal estimator with certain convergence guarantees, which can be implemented effectively in very modest processors, as an alternative to data-intensive DFT analysis. To investigate the feasibility of the approach, we set up a detailed physical simulation model (and presenting a solution to the associated Heat Equation on a relevant geometry) in a pseudo-online fashion and also test the proposed algorithm on data from a laboratory experiment. The initial results show promising performance, although refinements of the method are certainly possible.

The outline of the rest of the paper is as follows. Since it cannot be considered common knowledge to most readers in the Control community, Section II first outlines the basics of the 3ω method. Then Section III

[1] J. Bendtsen and J. Leth are with the Department of Electronic Systems, Aalborg University, Denmark (e-mail: dimon@es.aau.dk, jjl@es.aau.dk).

[2] C. Kallesøe is with the Department of Electronic Systems, Aalborg University, as well as Grundfos Management, Bjerringbro, Denmark (e-mail: ckallesoe@grundfos.com).

presents our main contribution, i.e., the aforementioned estimator. Section IV illustrates how the method works in simulation, while Section V presents its application to experimental data. Finally, Section VI summarizes the findings and provides some pointers to future work.

II. Preliminaries: the 3ω method

We consider the generic measurement setup shown in Figure 1. An electric heater element (orange) is fixed to a solid body (green), denoted substrate in the figure, and an alternating current is conducted through the heater by a current source.

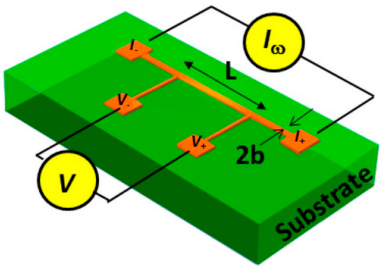

Fig. 1. Generic setup used in the 3ω method (from [8]).

While the heater is excited at a frequency ω, the periodic heating generates oscillations in the electrical resistance of the metal line at a frequency of 2ω. This phenomenon is then exploited to generate a voltage fluctuation in the heater at frequency 3ω, as explained by the following model description.

A. Heat Equation-based model

Consider the simplified geometric representation of the generic setup shown in Figure 2. Let $\chi \in \mathbb{R}^2$ denote 2D spatial coordinates as indicated in the figure, and let $\mathscr{H}$ and $\mathscr{S}$ denote the heater and substrate slab regions given in these coordinates, respectively. An alternating current of the form $I(t) = I_0 \cos \omega t$ is applied to the heater element, causing Joule heat generation of the form $P(t) = V(t)I(t)^2 = P_0(1+\cos 2\omega t)/4abk_h$, where $V(t)$ is the voltage drop across the heater caused by ohmic resistance, a and b are the width and thickness and k_h is the thermal conductivity of the heater element, respectively.

Assuming Joule heating in the heater element is the only source of thermodynamics in the system, we may then write up heat transfer equations for the regions $\mathscr{H}$, $\mathscr{S}$, and $\mathscr{A}$ as follows ([9]):

$$\frac{1}{\alpha_h}\frac{\partial T_h(\chi,t)}{\partial t} = \frac{\partial^2 T_h(\chi,t)}{\partial \chi_1^2} + \frac{\partial^2 T_h(\chi,t)}{\partial \chi_2^2} + \frac{P}{2abk_h}(1+\cos 2\omega t), \quad \chi \in \mathscr{H} \tag{1}$$

$$\frac{1}{\alpha_s}\frac{\partial T_s(\chi,t)}{\partial t} = \frac{\partial^2 T_s(\chi,t)}{\partial \chi_1^2} + \frac{\partial^2 T_s(\chi,t)}{\partial \chi_2^2}, \quad \chi \in \mathscr{S} \tag{2}$$

$$\frac{1}{\alpha_a}\frac{\partial T_a(\chi,t)}{\partial t} = \frac{\partial^2 T_a(\chi,t)}{\partial \chi_1^2} + \frac{\partial^2 T_a(\chi,t)}{\partial \chi_2^2}, \quad \chi \in \mathscr{A} \tag{3}$$

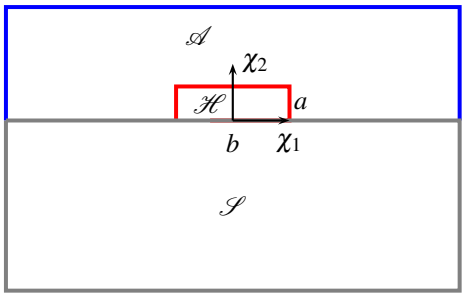

Fig. 2. Basic geometry for simulation of Joule heating.

Here, $T_h : \mathbb{R}^2 \times \mathbb{R}_+ \to \mathbb{R}$, $T_s : \mathbb{R}^2 \times \mathbb{R}_+ \to \mathbb{R}$, and $T_a : \mathbb{R}^2 \times \mathbb{R}_+ \to \mathbb{R}$ are the temperatures of the heater, substrate and ambient regions at spatial location χ and time t, respectively, and α_h, α_s, and α_a are the corresponding thermal diffusivities, respectively.

At the adiabatic boundaries of the heater, the normal derivative of T_h should vanish. For the substrate, at the isothermal boundaries we require that the temperature variation vanishes, while at the adiabatic boundaries the normal derivative must be zero. At the interface between the heater and the substrate/ambient, the temperature field is required to be continuous due to direct contact between the bodies (ambient medium).

Returning to the Joule heating, since voltage V is given as the product of the resistance of the wire R and the current I through it, multiplication of the sinusoidal current at the input frequency ω by the heater resistance fluctuations at 2ω results in a total voltage signal at the first and third harmonics (1ω and 3ω), which can be used to infer the magnitude of the temperature oscillations:

$$\begin{aligned} V(t) &= I(t)R(T_h(t)) = I_0 e^{\mathrm{i}\omega t}\left(R_0 + \frac{\partial R}{\partial T}\Delta T_h\right) \\ &= I_0 R_0 e^{\mathrm{i}\omega t} + I_0 C_0 e^{\mathrm{i}3\omega t} \end{aligned} \tag{4}$$

where C_0 is a constant and $\partial R/\partial T$ is a first-order approximation of the heater's rate of change in resistance with respect to changes in temperature.

B. Measurement method

Together with (1)–(3), (4) provides the theoretical basis for the 3ω method. Assuming the heater cross-section to be very small compared to the substrate cross-section and located at $\chi = 0$ and the heat being conducted to the substrate only—which is typically the case if the ambient is air, for example—(1)–(3) may be solved to yield a rather complicated integral expression for the heater temperature ([2]) involving the thermal conductivity of the substrate k_s. If the ambient medium is a good heat conductor such as water, k_s can be replaced by the thermal conductivity of that medium.

Fortunately, at low frequencies such that $2\omega b^2/\alpha_s \ll 1$, the aforementioned integral can be simplified as

$$\Delta T_h = \frac{P}{l\pi k_s}\left(-\frac{1}{2}\ln(\omega) + 0.923 - \mathrm{i}\frac{\pi}{4}\right) \tag{5}$$

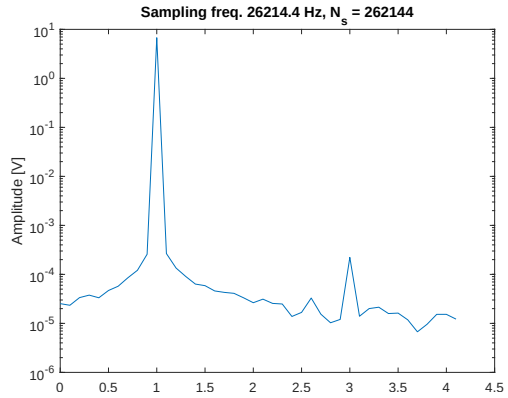

Fig. 3. Frequency spectrum generated from (4) in combination with (1)–(3)

where l is the length of the heater [1], [6]. The thermal conductivity k_s may thus be determined by the linear slope of a ΔT vs. $\ln\omega$ curve. However, as was noted in [1], the amplitude of the temperature oscillations can be expressed by the simple ratio

$$\Delta T_h \propto \frac{V_{3\omega}}{V_{1\omega}} \tag{6}$$

where $V_{1\omega}$ and $V_{3\omega}$ are, essentially, the two summands in (4). Knowing the proportionality factor in (6) ratio between the amplitudes of $V_{3\omega}$ and $V_{1\omega}$ thus allows us to isolate k_s in (5). This is traditionally done by applying a pure-tone sinusoidal current to the heater and measuring the generated voltage. Figure 3 shows an example of a frequency spectrum computed from the model (1)–(4), based on 2^{18} noisy samples acquired at a sampling frequency of approximately 26 kHz. The desired ratio the ratio $V_{3\omega}/V_{1\omega}$ is then read as the ratio between the peaks in the frequency spectrum; Notice that the resolution of such a frequency spectrum, and thus a precise estimate of $V_{3\omega}/V_{1\omega}$, relies on a high number of samples, as well as a sampling rate that is much higher than 3ω.

III. Time-domain estimator

This section describes the main contribution of the paper: a time-domain 3ω estimator aimed at extracting the temperature variations of the wire due to varying supply current. We wish to implement the algorithm on small micro-controllers with inexpensive components; however, since such devices often incorporate less than ideal oscillator crystals, we cannot trust the sampling frequency to be completely constant. Yet, in order to determine 1ω and 3ω frequencies reliably, it is important that the signal generation and voltage sampling are accurately synchronized. We propose to deal with this problem by generating the driving current reference i in the same micro-controller that is used for the signal analysis, meaning that the sampling time variations due to crystal uncertainties are at least identical for the signal generation and the measured samples.

A. Proposed estimator

The voltage relation (4) can be represented as the linear system

$$\dot{\zeta}(t) = \begin{bmatrix} 0 & \omega & 0 & 0 \\ -\omega & 0 & 0 & 0 \\ 0 & 0 & 0 & 3\omega \\ 0 & 0 & -3\omega & 0 \end{bmatrix} \zeta(t), \qquad \zeta(0) = \zeta_0 \tag{7}$$

$$V(t) = \begin{bmatrix} I_0 R_0 & 0 & c & 0 \end{bmatrix} \zeta(t) \tag{8}$$

with $\zeta \in \mathbb{R}^4$ and ζ_0 being a non-zero initial state. The coefficient $c \in \mathbb{R}_+$ is unknown, as discussed in the previous section, and must be estimated from sampled data.

Sampling the system (7)–(8) with sampling time τ and rescaling yields an observable discrete-time system of the form

$$z_{k+1} = \begin{bmatrix} A_1 & 0 \\ 0 & A_3 \end{bmatrix} z_k, \qquad z_0 = \frac{1}{I_0 R_0}\zeta_0 \tag{9}$$

$$y = \begin{bmatrix} 1 & 0 & d & 0 \end{bmatrix} z_k \tag{10}$$

where

$$\begin{aligned} A_n &= \exp \begin{bmatrix} 0 & n\omega\tau \\ -n\omega\tau & 0 \end{bmatrix} \\ &= \begin{bmatrix} \cos n\omega\tau & \sin n\omega\tau \\ -\sin n\omega\tau & \cos n\omega\tau \end{bmatrix}, \quad n \in \{1,3\} \end{aligned}$$

and $d \in \mathbb{R}_+$ is to be determined.

The current reference is generated by the following system implementation:

$$x_{k+1} = A_1 x_k + \kappa x_k (x_k^T x_k - 1) \tag{11}$$

$$i_k = \begin{bmatrix} 1 & 0 \end{bmatrix} x_k \tag{12}$$

which may, of course, be amplified as appropriate to match the sensitivity of the measurement equipment at hand. The signal generator (11) is chosen because it is highly robust to numerical errors; continued evaluations of trigonometric functions might accumulate inaccuracies over time due to small inaccuracies caused by, for example, finite word length of the processor hardware, but as will be shown below, the nonlinear term in (11) ensures that the signal generator continues to generate steady-state sinusoidal output signals with the fixed frequency ω regardless of running time.

The discrete-time voltage state is then identified by a state observer of the form

$$\hat{z}_{k+1} = \begin{bmatrix} A_1 & 0 \\ 0 & A_3 \end{bmatrix} \hat{z}_k + L(v_k - C z_k) \tag{13}$$

where v_k denotes the k'th voltage sample, L is a constant gain that renders the estimator stable (which is always possible to find, since (9)–(10) is always observable), and $C = \begin{bmatrix} 1 & 0 & 1 & 0 \end{bmatrix}$.

The ratio between the first and third harmonics is then given by

$$d = \frac{\|\hat{z}_k^{(3)}\|}{\|\hat{z}_k^{(1)}\|}$$

where $\hat{z}_k^{(1)}$ and $\hat{z}_k^{(3)}$ denote the first and third element of the state estimate, respectively.

B. Signal generator convergence to unit circle

To substantiate our claim that the proposed current generator remains numerically stable over time, we now show that by choosing κ appropriately, the sequence $\{x_k\}_{k\geq 0}$ defined by (11) can be made to approach the unit circle $\mathbb{S}\subset\mathbb{R}^2$ from any non-zero initial state.

Theorem 1: Consider the system (11). Let $x_0\neq 0$ be given, and choose κ such that

$$\max\left\{\frac{-1}{2|\gamma|},\frac{-\gamma+\sqrt{\gamma^2-1+\|x_0\|^{-2}}}{\|x_0\|^2-1}\right\}\leq\kappa<0 \qquad (14)$$

with $\gamma=\cos(\omega\tau)$. Then $\|x_{k+1}-A_1x_k\|\to 0$ and $\|x_k\|\to 1$ as $k\to\infty$.

Proof: Note first that if $\|x_k\|=1$ then $\|x_{k+1}\|=1$ for all k, since $A\in\mathrm{SO}(2)$. That is, independently of the choice of κ, if any element of the sequence $\{x_k\}_{k\geq 0}$ is an element of $\mathbb{S}$, then the entire sequence is contained in $\mathbb{S}$.

Next, let $a=\kappa(\|x_k\|^2-1)$ and note that

$$\begin{aligned}\|x_{k+1}\|^2&=x_k^T(A_1+aI)^T(A_1+aI)x_k\\&=x_k^T(I+2caI+a^2I)x_k\\&=(1+2ca+a^2)\|x_k\|^2.\end{aligned}$$

Hence

$$\|x_{k+1}\|=\sqrt{1+2ca+a^2}\|x_k\|. \qquad (15)$$

Now consider the case $\|x_k\|>1$. We wish to ensure that the sequence $\{x_k\}_{k\geq 0}$ approaches $\mathbb{S}$ while maintaining a norm strictly bigger than one for every element. To achieve this, we will need to choose κ such that a satisfies

$$\frac{1}{\|x_k\|^2}\leq 1+2\gamma a+a^2<1$$

which, by direct calculations, is satisfied whenever

$$-2\gamma<a\leq-\gamma-\sqrt{\gamma^2-1+\|x_k\|^{-2}} \qquad (16)$$

or

$$-\gamma+\sqrt{\gamma^2-1+\|x_k\|^{-2}}\leq a<0. \qquad (17)$$

From (17) we therefore get the requirement

$$\frac{-\gamma+\sqrt{\gamma^2-1+\|x_k\|^{-2}}}{\|x_k\|^2-1}\leq\kappa<0. \qquad (18)$$

Note that the left-hand side of (18) is a continuous, strictly increasing negative function of $\|x_k\|$ on the interval $(0,\infty)$, asymptotically approaching 0 for $\|x_k\|\to\infty$ (attaining the value $\frac{-1}{2|\gamma|}$ at $\|x_k\|=1$). Hence, the sequence $\{x_k\}_{k\geq 0}$ will approach $\mathbb{S}$ if $\|x_0\|>1$ and κ is chosen according to (18) with $k=0$.

For the case $\|x_k\|<1$, we proceed in a similar way as the above and choose a such that

$$\frac{1}{\|x_k\|^2}\geq 1+2\gamma a+a^2>1,$$

which is satisfied whenever

$$-2\gamma>a\geq-\gamma-\sqrt{\gamma^2-1+\|x_k\|^{-2}} \qquad (19)$$

or

$$-\gamma+\sqrt{\gamma^2-1+\|x_k\|^{-2}}\geq a>0 \qquad (20)$$

from which we recover (18) when using (20), and therefore get the requirement

$$\frac{-1}{2|\gamma|}\leq\kappa<0 \qquad (21)$$

since in this case the left-hand side of (18) is bounded above by $\frac{-1}{2|\gamma|}$. Hence, in this case the sequence $\{x_k\}_{k\geq 0}$ will approach $\mathbb{S}$ if $\|x_0\|<1$ and κ is chosen according to (21).

In summary we conclude that by choosing κ as stated in (14) will ensure that the sequence $\{x_k\}_{k\geq 0}$ approaches $\mathbb{S}$ as k tends to infinity. That is, $\|x_k\|^2\to 1$ and hence $\|x_{k+1}-A_1x_k\|\to 0$ as $k\to\infty$. ■

A few remarks are in order. Firstly, it is pointed out that the sampling time τ should be chosen sufficiently fast that effective estimation of the signal amplitudes at 1ω and 3ω is possible, i.e., τ should be chosen significantly smaller than $1/6\omega$ according to the Nyquist-Shannon sampling theorem. This implies that κ must satisfy $\cos(1/6)<0.9862<\gamma<1$, which can be used to obtain a quick estimate of the possible range of κ.

Secondly, it is noted that (14) is strictly a sufficient condition; it is possible to find other values of κ that causes $\{x_k\}_{k\geq 0}$ to approach the unit sphere (e.g.. using (16) and (19)). However, finding a complete classification of all such κ appears to be a very complex undertaking due to the discrete-time setting, and not really needed for our purpose in this paper.

And thirdly, although at first glance the point about $\|x_{k+1}-Ax_k\|\to 0$ appears trivial, it is actually useful as it shows that the state behaves like a perfect harmonic oscillator, rotating on the unit circle with a constant angular frequency. Small numerical deviations will be kept in check by the attraction to the unit circle, rather than accumulating over time.

IV. Simulation results

To test the implementation with the combined signal generator (11) and the state estimator (13), a simulation in which the distributed parameter model (1)–(4) is combined with (11)–(12) and (13), is executed. The simulation is implemented in MatLab using the Partial Differential Equation toolbox in a sampled-data fashion; at every sample instant, (11)–(12) first generates a current sample, then (1)–(4) are integrated in "pseudo-continuous time" using the nonlinear PDE solver provided by the MatLab toolbox for one sampling period, the average heater temperature is computed, and the resulting voltage is computed from (4). The sampling rate is chosen to 102 Hz, and material parameters are taken to simulate platinum, silicon carbide, and air for

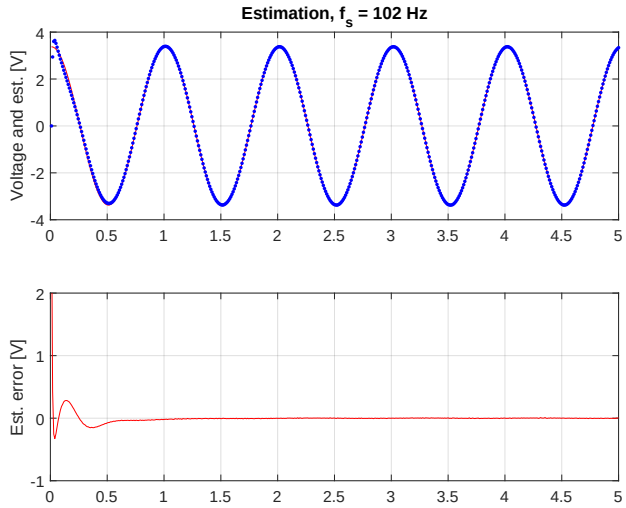

Fig. 4. Time series data showing state estimate convergence (top) and estimation error (bottom).

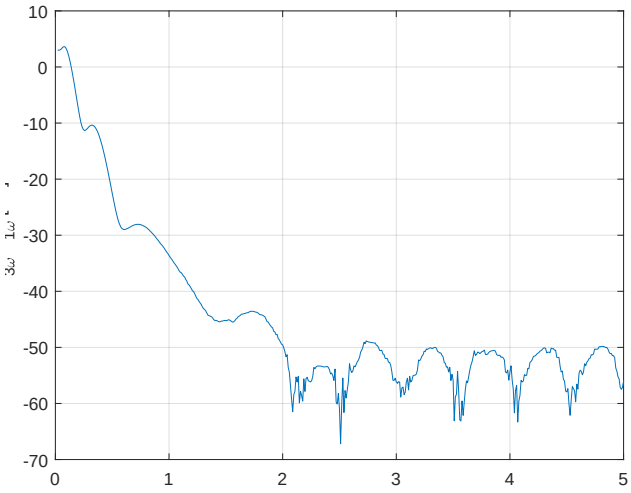

Fig. 5. Ratio $\|\hat{z}_k^{(3)}\|/\|\hat{z}_k^{(1)}\|$ evaluated at each sample instant.

heater, substrate and ambient, respectively. Figures 5 and 6 show the state estimate convergence and $V_{3\omega}/V_{1\omega}$ estimation, respectively.

From Figure 4, it is clear that the estimate converges in less than one second in the noise-free case. Figure 5 shows that the $V_{3\omega}/V_{1\omega}$ ratio has converged to a general steady-state level after about two seconds. An offline DFT analysis gives a ratio of -62 dB, indicating that the filter-based estimation is best when the voltage amplitude is at the peak value(s).

V. Test Results

The state estimation approach is tested on data sets obtained from laboratory experiments carried out at the Department of Biology, Aalborg University. Here, experiments with a platinum wire with length of 2.5 cm and diameter 20 μm (Goodfellow, PT00-WR-000110)

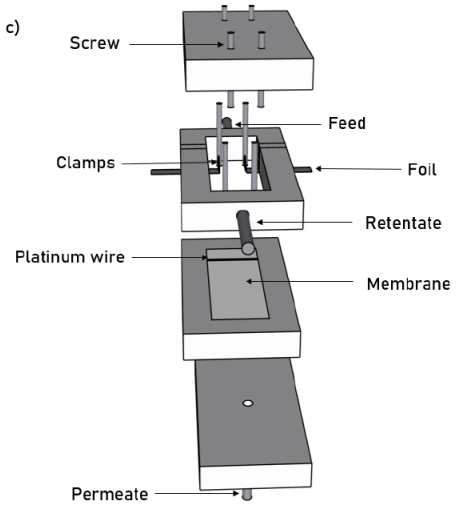

Fig. 6. Sketch of laboratory setup.

TABLE I
First and third harmonic amplitude of the measured voltage and their ratio.

Data set	$V_{1\omega}$	$V_{3\omega}$	$V_{3\omega}/V_{1\omega}$ [dB]
Pure water	0.51 V	0.483 mV	-60.4
Incipient fouling	0.50 V	0.406 mV	-61.8
Severe fouling	0.49 V	0.623 mV	-57.9
Pure air	0.53 V	12.0 mV	-32.8

was exposed to different conditions, see Figure 6. The supply current was supplied by a Keithley Model 6221 AC/DC current source. For the data acquisition, a 16-bit 250 kS/s National Instruments USB-6210 data aquisition card was used. The sampling frequency was 20 kHz.

The wire was exposed to

- pure water.
- incipient fouling on the membrane.
- severe fouling on the membrane.
- pure air.

To establish a baseline for the evaluation of the state observer, the frequency content of the measured voltage is analyzed. The frequency analysis leads to first and third harmonic shown in Table I.

In control theory it is recommended as a rule of thumb to sample a signal with between 6 and 40 time faster than the fastest frequency in the system [10, p. 485]. With a supply current frequency of 1 Hz it means that the highest expected frequency in the voltage signal is 3 Hz, hence a sampling frequency of around 90 Hz should be a good choice. The data from the lab tests are therefore down-sampled to agree with this sampling frequency to show that the state observer is able to operate with this lower sampling rates.

The results with the state observer is shown in Fig. 7. The first plot shows the estimated amplitude of the first harmonic, the second plot shows the third harmonic, and

the last plot shows the ratio between $V_{3\omega}$ and $V_{1\omega}$ in dB. Along with the state estimation obtained by the observer, the damping from Table I calculated from the frequency analysis are shown with dashed lines in the last plot. It is clear that the observer is able to obtain good estimates of the damping, yielding a damping ratio very close to what a DFT analysis yields. Furthermore, it is able to do so with a much lower sampling frequency based on 15 seconds of samples. The oscillations that happens in the pure water case is due to a slowly varying offset on the measured voltages, which may in principle be removed by high-pass filtering; however, for the sake of clarity in the presentation no filtering is performed in this study.

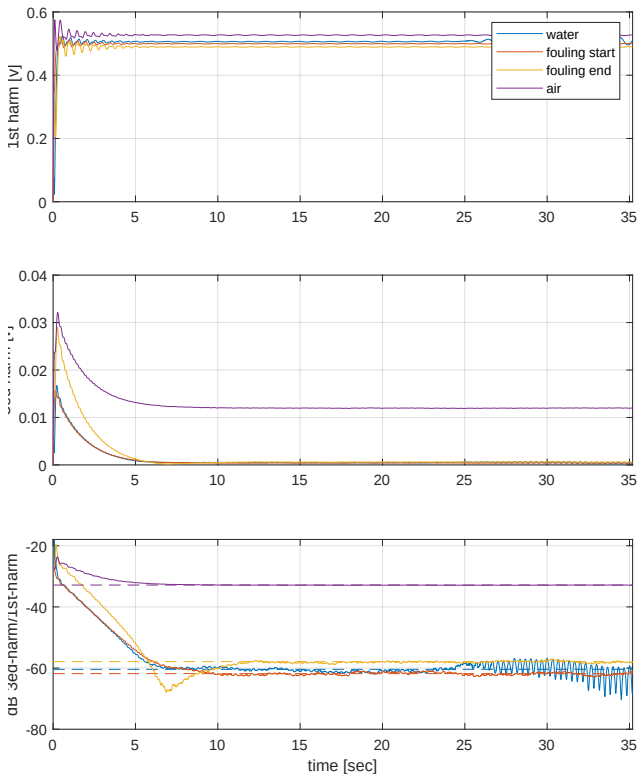

Fig. 7. First and third harmonic estimated by the state observer and the ratio between them. The damping of the third harmonic calculated from the frequency analysis (dashed lines in the last plot) is shown along with the ratio estimated by the state observer is shown in the last plot.

VI. Conclusion

In this paper we proposed a novel approach to the so-called 3ω method for measuring thermal conductivity. The 3ω method is a frequency-based method, in which the ratio between the first and third harmonics of an induced voltage in an electric heater element can be shown to be (inversely) proportional to the thermal conductivity of the solid or fluid that the heater is in contact with. The key feature of the proposed approach is that, due to its modest memory and sampling rate requirements, it can be implemented in a cheap micro-controller and therefore likely to be useful for feedback in control loops or similar applications.

The approach comprises two main elements, a discrete-time signal generator that provides a steady-state sinusoidal current output, and a standard Luenberger-style state observer designed to estimate the associated third harmonic in the presence of noisy voltage measurements. The approach was tested in simulation and on actual laboratory data, showing good agreement with traditional off-line analysis. We see potential usage of the method in applications such as detection of fouling in membrane filtering processes, water level sensing, slow flow measurements etc.

The work presented in this paper is only the first step to introducing the idea. The immediate first step is obviously to implement the algorithm in an actual micro-processor and test it online. Further, it will also be necessary to investigate more rigorously how low sampling frequencies can be tolerated, how finite word length influences the $V_{3\omega}/V_{1\omega}$ ratio, as well as how to tune the state observer to obtain fast convergence.

ACKNOWLEDGMENT

The authors would like to extend their sincere gratitude to Astrid Kjul, Louise Mikkelsen, Maiken Poulsen, Simon Hansen, Pernille Jensen, Jacob Andersen, Nikitha Thavaneswaran (Group Bio-21-BT-5-4 at the Department of Chemistry and Bioscience, Aalborg University), and their supervisor Mads K. Jørgensen, for granting access to their experimental data.

References

[1] D. Cahill and R. Pohl, "Thermal conductivity of amorphous solids above the plateau," Physical Review B, vol. 35, no. 8, pp. 4067–4073, 1987.

[2] D. Cahill, "Thermal conductivity measurement from 30 to 750 k: the 3ω method," Review of Scientific Instruments, vol. 61, pp. 802–808, 1990.

[3] N. O. Birge and S. R. Nagel, "Wide-frequency specific heat spectrometer," Review of Scientific Instruments, vol. 58, no. 8, pp. 1464–1470, 1987.

[4] J. Moon, Y. Jeong, and S. Kwun, "The 3ω technique for measuring dynamic specific heat and thermal conductivity of a liquid or solid," Review of Scientific Instruments, vol. 67, pp. 29–35, 1996.

[5] R. Bernhardsgrutter, C. Hepp, K. Schmitt, M. Jagle, H.-F. Pernau, and J. Wollenstein, "Robust and flexible thermal sensor using the 3-omega-method to investigate thermal properties of fluids," in Proc. of Transducers 2019 and Eurosensors XXXIII, 2019.

[6] C. Clausen, T. Pedersen, and A. Bentien, "The 3-omega method for the measurement of fouling thickness, the liquid flow rate, and surface contact," Sensors, vol. 17, no. 552, 2017.

[7] D.-W. Oh, "Analysis on measurement of hydrogen concentration in air mixture using 3 omega method," International Journal of Nanotechnology, vol. 19, pp. 88–93, 2022.

[8] W. Jaber and P.-O. Chapuis, "Non-idealities in the 3ω method for thermal characterization in the low- and high-frequency regimes," AIP Advances, vol. 8, 2018.

[9] H. Wang and M. Sen, "Analysis of the 3-omega method for thermal conductivity measurement," International Journal of Heat and Mass Transfer, vol. 52, pp. 2102–2109, 2009.

[10] G. Franklin, J. Powell, and M. Workman, Digital Control of Dynamic Systems - second edition. Addison-Wesley, 1990.